Velocity and Temperature Streaming in Oscillating Boundary Layers

Demetri P. Telionis* and Maria S. Romaniuk†
Virginia Polytechnic Institute and State University, Blacksburg, Va.

A method is described for integration of the incompressible, laminar, boundary-layer equations with periodic fluctuating outer-flow velocity and temperature distributions. The method is a combination of numerical analysis and perturbation techniques and is valid for small amplitude ratios ϵ. It is demonstrated that a reduction by at least a factor of one hundredth in computer storage is accomplished in comparison with methods that solve numerically the governing equations. Temperature distributions and heat transfer rates are studied and the effect of dissipation on the fluctuation is included for the first time. Steady streaming components of velocity, temperature, and heat transfer are also investigated. Such phenomena may appear quite significant in re-entry aerodynamics where dissipation plays a significant role.

I. Introduction

VELOCITY fields that fluctuate about a mean are very common in practice and quite often the amplitude of oscillations is relatively small, for example in flows through cascades of turbomachinery or over helicopter rotor blades. Investigations of such flowfields hinge on accurate solutions of the boundary-layer equations. It is the nonlinearity of these equations that makes the problem intriguing and generates peculiar effects, some of which will be described in the present paper. Work in this area had been initiated in the 1950's by Moore,[1] Lighthill,[2] and Lin.[3] The literature has been surveyed critically and the reader can find extensive accounts of earlier publications on the topic in recent review articles.[4-6] In the present paper, we will only briefly outline the various methods of attack.

The work in this area can be grouped, according to the methodology followed, into three major categories. Contributions of the first category[7-10] are based on an asymptotic expansion in powers of the amplitude parameter ϵ and the frequency parameter $\omega x/U_\infty$, where ω is the frequency, x is the distance along the wall, and U_∞ is a typical velocity of the outer flow. This method was originally suggested by Lighthill[2] and has been followed by most of the subsequent investigators. However, almost all the work that followed along these lines is confined to very simple body configurations of only academic importance and extreme values of the frequency. The second category includes exact numerical solutions[11,12] in three coordinates: two space variables and time. The computer space and time required by such methods are relatively high and, as a result, routine calculations became possible only in the last decade. As a third method of approach, we consider the method of averaging, which is valid only for large frequencies but can be used to treat arbitrary amplitudes of oscillations. This promising method was proposed by Lin,[3] but, to the knowledge of the authors, it has not been developed further since then.

A method that combines the advantages of the first two categories, the asymptotic expansions and the numerical analysis, has been employed by the present authors.[13] This paper is an extension of Ref. 13. Dependent variables are expanded in terms of a small amplitude parameter and the resulting equations are solved numerically in the two-dimensional space. In this way we are not confined to trivial body configurations or extreme values of the frequency parameter. On the other hand, our numerical integration is performed in a two-coordinate space. This requires storage that corresponds only to a few x stations rather than the entire x-y plane, where x and y are the coordinates parallel and perpendicular to the solid boundary, respectively. We thus combine, in a way, the simplicity of the methods of the first category with the versatility of the methods of the second category. It is strongly believed that only a method like the present one could be extended to three-dimensional space configurations. All other methods of numerical analysis would require storage of information at all the points of a three-dimensional mesh.

Heat transfer effects in oscillating boundary layers were studied first by Moore[1] and Lighthill.[2] Moore[1] and later Moore and Ostrach[14] investigated the deviations from the quasisteady flow, while Ostrach[15] considered a steady flow and assumed slow fluctuations of the wall temperature. Heat transfer rates were also calculated by Sparrow and Gregg,[16] King,[17] and Telionis and Gupta,[18] but only for self-similar mean flows.

Our analysis in Ref. 13 and here is carried up to order ϵ^2. We thus capture nonlinear streaming effects that had been indentified before only by virtue of other methods.[3,12] We then proceed to study, for the first time, the effects of nonlinear streaming on the temperature field and heat transfer.

A point that has surprisingly slipped the attention of all the investigators until very recently[4] is the validity of the boundary-layer approximation at the levels of order ϵ or ϵ^2. An analysis of the validity of the boundary-layer approximation in calculating oscillatory and steady streaming contributions to the velocity and temperature fields is performed. Numerical results are provided to demonstrate the necessity of such considerations.

II. Governing Equations

We assume here that for large Reynolds numbers, the effects of viscosity are confined to thin layers, adjacent to the solid boundaries; a fact that has been verified analytically and experimentally. In other words, we admit that the flowfield can be described by the Euler equations, except for a thin layer, in which the full Navier-Stokes equations will have to be employed. Matching the two solutions will require, in

Presented as Paper 77-235 at the AIAA 15th Aerospace Sciences Meeting, Los Angeles, Calif., Jan. 24-26, 1977; submitted July 13, 1977; revision received Dec. 16, 1977.

Index category: Boundary Layers and Convective Heat Transfer—Laminar.

*Associate Professor, Dept. of Engineering Science and Mechanics. Associate Fellow AIAA.

†Graduate Research Assistant. Member AIAA.

general, matching of velocity, temperature, pressure, and their slopes at an interface whose location will be determined as part of the solution. The equations that govern the incompressible flow in the viscous layer are:

$$\frac{\partial u}{\partial x}+\frac{\partial v}{\partial y}=0 \tag{1}$$

$$\frac{\partial u}{\partial t}+u\frac{\partial u}{\partial x}+v\frac{\partial u}{\partial y}=-\frac{1}{\rho}\frac{\partial p}{\partial x}+\nu\left(\frac{\partial^2 u}{\partial x^2}+\frac{\partial^2 u}{\partial y^2}\right) \tag{2}$$

$$\frac{\partial v}{\partial t}+u\frac{\partial v}{\partial x}+v\frac{\partial v}{\partial y}=-\frac{1}{\rho}\frac{\partial p}{\partial y}+\nu\left(\frac{\partial^2 v}{\partial x^2}+\frac{\partial^2 v}{\partial y^2}\right) \tag{3}$$

$$\frac{\partial T}{\partial t}+u\frac{\partial T}{\partial x}+v\frac{\partial T}{\partial y}=\alpha\left(\frac{\partial^2 T}{\partial x^2}+\frac{\partial^2 T}{\partial y^2}\right)+\frac{\nu}{c}\Phi \tag{4}$$

where x, y, and u, v are the coordinates and velocity components parallel and perpendicular to the wall, respectively; t, p, ρ, ν, c, and α are the time, pressure, density, kinematic viscosity, specific heat, and thermal diffusivity, respectively; and $\Phi=2(\partial u/\partial x)^2+2(\partial v/\partial y)^2+(\partial u/\partial y+\partial v/\partial x)^2$.

The boundary conditions at the wall require that

$$u=v=o \text{ and } T=T_w \text{ at } y=0 \tag{5}$$

where T_w is the temperature of the wall. At the outer edge of the viscous layer, we require that the velocity and temperature match the inviscid field

$$u=U_e,\ v=V_e,\ T=T_e, \text{ and } p=p_e \text{ at } y=\delta \tag{6}$$

where e denotes the outer edge values of the quantities and δ is the thickness of the viscous layer. The velocity and temperature thicknesses are not equal, in general, but this will not affect the calculations that are performed in the stretched boundary-layer type system of coordinates.

We are interested here in the response of the viscous layer to periodic fluctuations of the outer flow, given in the most general form by

$$U_e(x,t)=U_0(x)+\left[\frac{\epsilon}{2}U_1e^{i\omega t}+\frac{\epsilon^2}{2}U_2e^{2i\omega t}+\ldots+CC\right] \tag{7}$$

$$V_e(x,t)=V_0(x)+\left[\frac{\epsilon}{2}V_1e^{i\omega t}+\frac{\epsilon^2}{2}V_2e^{2i\omega t}+\ldots+CC\right] \tag{8}$$

$$p_e(x,t)=p_{e0}(x)+\left[\frac{\epsilon}{2}p_{e1}e^{i\omega t}+\frac{\epsilon^2}{2}p_{e2}e^{2i\omega t}+\ldots+CC\right] \tag{9}$$

$$T_e(x,t)=T_{e0}(x)+\left[\frac{\epsilon}{2}T_{e1}e^{i\omega t}+\frac{\epsilon^2}{2}T_{e2}e^{2i\omega t}+\ldots+CC\right] \tag{10}$$

where U_i, V_i, T_{ei}, P_{ei} are functions of x only, CC denotes the complex conjugate of the preceding expression, ϵ is a small dimensionless parameter, and ω is the frequency of the fluctuation. The method presented can be used to study the effects of second harmonics, but of all the terms of $0(\epsilon^2)$ only the steady corrections to velocity and temperature profiles will be of concern here. These corrections, representing streaming phenomena, are independent of the higher harmonics. It should be noted further that if the quantities U_i, V_i, and T_{ei} with $i=1, 2,\ldots$ are complex, then Eqs. (7-10) represent a general periodic motion with phase differences between the velocity components and temperature.

III. Perturbations

We will seek solutions to Eqs. (1-4), subject to the boundary conditions given by Eqs. (7-10), in the form

$$q(x,y,t)=q_0(x,y)+(\epsilon/2)[q_1(x,y)e^{i\omega t}+CC]$$
$$+\epsilon^2[\tfrac{1}{2}q_2(x,y)e^{2i\omega t}+CC+q_s(x,y)]+\ldots \tag{11}$$

where q represents any of the four unknown field quantities u, v, T, and p. The streaming terms u_s, v_s, and T_s are included in the expansion in order to balance the nonlinear steady contributions that appear in the equations of order ϵ^2. For more details, the reader is referred to Ref. 13.

Substituting Eqs. (7-11) into Eqs. (1-4) and collecting terms of order ϵ° we get

$$\frac{\partial u_0}{\partial x}+\frac{\partial v_0}{\partial y}=0 \tag{12}$$

$$u_0\frac{\partial u_0}{\partial x}+v_0\frac{\partial u_0}{\partial y}=-\frac{1}{\rho}\frac{\partial p_0}{\partial x}+\nu\left(\frac{\partial^2 u_0}{\partial x^2}+\frac{\partial^2 u_0}{\partial y^2}\right) \tag{13}$$

$$u_0\frac{\partial v_0}{\partial x}+v_0\frac{\partial v_0}{\partial y}=-\frac{1}{\rho}\frac{\partial p_0}{\partial y}+\nu\left(\frac{\partial^2 v_0}{\partial x^2}+\frac{\partial^2 v_0}{\partial y^2}\right) \tag{14}$$

$$u_0\frac{\partial T_0}{\partial x}+v_0\frac{\partial T_0}{\partial y}=\alpha\left(\frac{\partial^2 T_0}{\partial x^2}+\frac{\partial^2 T_0}{\partial y^2}\right)+\frac{\nu}{c}\Phi_0 \tag{15}$$

where $\Phi_0=2(\partial u_0/\partial x)^2+2(\partial v_0/\partial y)^2+(\partial u_0/\partial y+\partial v_0/\partial x)^2$, subject to the boundary conditions derived from Eqs. (5) and (6)

$$u_0=v_0=0,\quad T_0=T_{w0} \text{ at } y=0 \tag{16}$$

$$u_0=U_0,\ v_0=V_0,\ T_0=T_{e0},\ p_0=p_{e0} \text{ at } y=\delta \tag{17}$$

At this point we recover the steady-state equations, regardless of the value of the frequency.

We choose now the freestream velocity U_∞, temperature difference T_w-T_∞, and a typical length of the body configuration L as characteristic dimensions, in order to bring the preceding set of equations to their boundary-layer form. Within an error of order R_0^{-1}, where $R_0=U_\infty L/\nu$ is the Reynolds number, the pressure across the boundary layer may be considered constant and Bernoulli's equation can be used to determine p_0.

We thus have

$$\frac{\partial u_0}{\partial x}+\frac{\partial \tilde{v}_0}{\partial \tilde{y}}=0 \tag{*18}$$

$$u_0\frac{\partial u_0}{\partial x}+\tilde{v}_0\frac{\partial u_0}{\partial \tilde{y}}=U_0\frac{dU_0}{dx}+\frac{\partial^2 u_0}{\partial \tilde{y}^2}+\frac{1}{R_0}\frac{\partial^2 u_0}{\partial x^2} \tag{*19}$$

$$u_0\frac{\partial T_0}{\partial x}+\tilde{v}_0\frac{\partial T_0}{\partial \tilde{y}}=\frac{1}{Pr}\left(\frac{\partial^2 T_0}{\partial \tilde{y}^2}+\frac{1}{R_0}\frac{\partial^2 T_0}{\partial x^2}\right)+Ec\left\{\left(\frac{\partial u_0}{\partial \tilde{y}}\right)^2\right.$$
$$\left.+\frac{2}{R_0}\left[\left(\frac{\partial u_0}{\partial x}\right)^2+\left(\frac{\partial \tilde{v}_0}{\partial \tilde{y}}\right)^2+\frac{\partial u_0}{\partial \tilde{y}}\frac{\partial \tilde{v}_0}{\partial x}\right]+\left(\frac{1}{R_0}\frac{\partial \tilde{v}_0}{\partial x}\right)^2\right\} \tag{*20}$$

where $Pr=\nu/\alpha$ and $Ec=U^2/c(T_w-T_\infty)$ are the Prandtl and Eckert numbers, respectively. In the preceding equations, we have retained the same symbols to denote dimensionless quantities. Moreover, the symbol T represents the dimensionless deviation from the temperature of the outer stream $(T-T_\infty)/(T_w-T_\infty)$. Whenever there is danger of confusion, we will mark equations expressed in terms of dimensionless quantities by a asterisk in front of the equation number. The tilde over v and y denotes stretched variables.

$$\tilde{v}_0 = R_0^{1/2} v_0 \qquad \tilde{y} = R_0^{1/2} y \qquad *(21)$$

Neglecting terms of order R_0^{-1}, we obtain the classical set of boundary-layer equations for incompressible steady flow. The appropriate boundary conditions are then

$$u_0 = v_0 = 0 \text{ and } T_0 = 1 \text{ at } \tilde{y} = 0 \qquad *(22)$$

$$u_0 = U_0 \text{ and } T_0 = 0 \text{ at } \tilde{y} \to \infty \qquad *(23)$$

where U_0 is now the value of the outer flow at $y = 0$ and the error thus committed is of order R_0^{-1}.

Collection of terms of order ϵ yields

$$\frac{\partial u_1}{\partial x} + \frac{\partial v_1}{\partial y} = 0 \qquad (24)$$

$$i\omega u_1 + u_0 \frac{\partial u_1}{\partial x} + u_1 \frac{\partial u_0}{\partial x} + v_0 \frac{\partial u_1}{\partial y} + v_1 \frac{\partial u_0}{\partial y} = -\frac{1}{\rho} \frac{\partial p_1}{\partial x} + \nu \left(\frac{\partial^2 u_1}{\partial x^2} + \frac{\partial^2 u_1}{\partial y^2} \right) \qquad (25)$$

$$i\omega v_1 + u_0 \frac{\partial v_1}{\partial x} + u_1 \frac{\partial v_0}{\partial x} + v_0 \frac{\partial v_1}{\partial y} + v_1 \frac{\partial v_0}{\partial y} = -\frac{1}{\rho} \frac{\partial p_1}{\partial y} + \nu \left(\frac{\partial^2 v_1}{\partial x^2} + \frac{\partial^2 v_1}{\partial y^2} \right) \qquad (26)$$

$$i\omega T_1 + u_0 \frac{\partial T_1}{\partial x} + u_1 \frac{\partial T_0}{\partial x} + v_0 \frac{\partial T_1}{\partial y} + v_1 \frac{\partial T_0}{\partial y} = \alpha \left(\frac{\partial^2 T_1}{\partial x^2} + \frac{\partial^2 T_1}{\partial y^2} \right) + \frac{\nu}{c} \left[4 \frac{\partial u_0}{\partial x} \frac{\partial u_1}{\partial x} + 4 \frac{\partial v_0}{\partial y} \frac{\partial v_1}{\partial y} + 2 \left(\frac{\partial u_0}{\partial y} + \frac{\partial v_0}{\partial x} \right) \left(\frac{\partial u_1}{\partial y} + \frac{\partial v_1}{\partial x} \right) \right] \qquad (27)$$

Equations (24-27) represent, in general, an elliptic disturbance to the parabolic field given by Eqs. (18-20) for $R_0 \to \infty$. It should be emphasized that Eqs. (18-20) can be solved by any marching technique. Equations (24-27) are linear and could be parabolized so that their solution could be derived simultaneously with the boundary-layer equations for the steady part of the flow. Solutions to these equations would require, of course, the proper boundary conditions for elliptic differential equations.

The solution to Eqs. (24-27) represents a Stokes layer whose thickness is of the order $(\nu/\omega)^{1/2}$, a quantity which is small for most practical applications. We may assume safely then, that the derivatives $\partial u_1/\partial x$ and $\partial u_1/\partial y$ scale like U_∞/L and U_∞/δ_1, respectively, where δ_1 is the thickness of the Stokes layer. The familiar procedure for deriving the boundary-layer equations can, therefore, be repeated, provided the quantity $R_1 = \omega L^2/\nu$ is large, in order to arrive at the following dimensionless form

$$\frac{\partial u_1}{\partial x} + \frac{\partial \tilde{v}_1}{\partial \tilde{y}} = 0 \qquad *(28)$$

$$i\omega u_1 + u_0 \frac{\partial u_1}{\partial x} + u_1 \frac{\partial u_0}{\partial x} + \tilde{v}_0 \frac{\partial u_1}{\partial \tilde{y}} + \tilde{v}_1 \frac{\partial u_0}{\partial \tilde{y}} = i\omega U_1 + U_0 \frac{\partial U_1}{\partial x} + U_1 \frac{\partial U_0}{\partial x} + \frac{\partial^2 u_1}{\partial \tilde{y}^2} + 0(1/R_1) \qquad *(29)$$

$$i\omega T_1 + u_0 \frac{\partial T_1}{\partial x} + u_1 \frac{\partial T_0}{\partial x} + \tilde{v}_0 \frac{\partial T_1}{\partial \tilde{y}} + \tilde{v}_1 \frac{\partial T_0}{\partial \tilde{y}} = \frac{\partial^2 T_1}{\partial \tilde{y}^2} + 2Ec \frac{\partial u_0}{\partial \tilde{y}} \frac{\partial u_1}{\partial \tilde{y}} + 0(1/R_1) \qquad *(30)$$

with the boundary conditions

$$u_1 = \tilde{v}_1 = 0, \quad T_1 = T_w \text{ at } \tilde{y} = 0 \qquad *(31)$$

$$u_1 = U_1, \quad T_1 = T_{1e} \text{ as } \tilde{y} \to \infty \qquad *(32)$$

The boundary conditions for T_1, in general, allow the temperatures at the wall and at the edge of the layer to fluctuate with the amplitudes T_{1w} and T_{1e}, respectively. In the preceding equations, the quantities ωL and L have been used to render velocities and lengths dimensionless, and R_1 was used for the stretching process. The dimensionless symbols in these equations, therefore, are not the same with the symbols of the dimensionless equations of zeroth order, i.e., Eqs. (18-20). The preceding boundary-layer approximation is valid only if the function $U_1(x)$ does not change sharply with x. Otherwise, the ratio U_∞/L is not a good estimate of the order of magnitude of the derivative $\partial u_1/\partial x$. This would be the case, for example, if the unsteadiness were induced in the outer flow by a control surface or if a wavelike disturbance with a wave length of the order of the boundary-layer thickness was traveling downstream.[4] Moreover, we should require that the solution of Eqs. (28-30) represent a more significant correction to the mean boundary-layer flow than the terms of order R_0^{-1} that we neglected there. That is, we require that $R_0 \gg \epsilon^{-1}$, a condition which appears not very restrictive. Note that the ratio of the thicknesses δ_0 and δ_1, of the mean and the fluctuating layers, respectively, is independent of the amplitude of the oscillations; that is, $\delta_1/\delta_0 = (U_\infty/\omega L)^{1/2}$.

IV. Nonlinear Streaming

Collecting the terms of order ϵ^2 in Eqs. (1-4), where u, v, T, and p are expressed in the form given by Eq. (11), we derive two sets of differential equations—one for the second harmonic amplitudes u_2, v_2, T_2, and one for the streaming terms u_s, v_s, T_s. The first set of equations can be used to estimate a correction to the unsteady part of the motion. This represents a distortion of the harmonic response due to the nonlinearity of the boundary-layer equations. The second set of equations gives the steady, second-order corrections. However, at this point we may have to account for the fact that terms of order R_0^{-1} that were neglected in Eqs. (18-20) may be comparable to the terms in the streaming equation if $R_0^{-1} = 0(\epsilon^2)$. Caution should be exercised in using a uniform nondimensionalization and stretching for equations of order ϵ^0 and ϵ^2. In their dimensionless boundary-layer form, the streaming equations are:

$$\frac{\partial u_s}{\partial x} + \frac{\partial \tilde{v}_s}{\partial \tilde{y}} = 0 \qquad *(33)$$

$$u_0 \frac{\partial u_s}{\partial x} + \tilde{v}_0 \frac{\partial u_s}{\partial \tilde{y}} + u_s \frac{\partial u_0}{\partial x} + \tilde{v}_s \frac{\partial u_0}{\partial \tilde{y}} = -\frac{1}{2} \mathcal{R}e \left[\tilde{u}_1 \frac{\partial u_1}{\partial x} + \tilde{v}_1 \frac{\partial u_1}{\partial \tilde{y}} \right] + \frac{U_1}{2} \frac{dU_1}{dx} + \frac{\partial^2 u_s}{\partial \tilde{y}^2} + \frac{1}{\epsilon^2 R_0} \frac{\partial^2 u_0}{\partial x^2} + \frac{1}{R_s} \frac{\partial^2 u_s}{\partial x^2} \qquad *(34)$$

$$u_0\frac{\partial T_s}{\partial x}+\bar{v}_0\frac{\partial T_s}{\partial \bar{y}}+u_s\frac{\partial T_0}{\partial x}+\bar{v}_s\frac{\partial T_0}{\partial \bar{y}}=\frac{1}{Pr}\left[\frac{\partial^2 T_s}{\partial \bar{y}^2}+\frac{1}{\epsilon^2 R_0}\frac{\partial^2 T_0}{\partial x^2}\right]-2\mathcal{R}e\left[\bar{u}_1\frac{\partial T_1}{\partial x}+\bar{\bar{v}}_1\frac{\partial T_1}{\partial \bar{y}}\right]$$

$$+Ec\left\{2\frac{\partial u_0}{\partial \bar{y}}\frac{\partial u_s}{\partial \bar{y}}+\frac{1}{2}\frac{\partial u_1}{\partial \bar{y}}\frac{\partial \bar{u}_1}{\partial \bar{y}}+\frac{2}{\epsilon^2 R_0}\times\left[\left(\frac{\partial u_0}{\partial x}\right)^2+\left(\frac{\partial \bar{v}}{\partial \bar{y}}\right)^2+\frac{\partial u}{\partial \bar{y}}\frac{\partial \bar{v}}{\partial x}\right]\right\}+0\left(\frac{1}{R_s}\right) \quad *(35)$$

with the homogeneous boundary conditions

$$u_s=v_s=T_s=0 \text{ at } \bar{y}=0 \quad *(36)$$

$$u_s=v_s=T_s=0 \text{ as } \bar{y}\to\infty \quad *(37)$$

$\mathcal{R}e$ stands for the real part of the expression that follows and an overbar denotes the complex conjugate. We notice here that the forcing terms $\bar{u}_1\,\partial u_1/\partial x+\bar{v}_1\,\partial u_1/\partial \bar{y}$ are similar to the terms that drive the streaming phenomenon in the case of zero mean flow. This problem has recently been extensively studied.[4-6] The terms on the left-hand side of Eq. (34) represent the convection effect due to the presence of the mean flow. Assuming that the order of magnitude of the streaming quantities is not greatly affected by the mean flow, that is the left-hand side of Eq. (34), we can make use of Stuart's estimates. Stuart[4] pointed out that the streaming phenomena do not disappear at the edge of the Stokes layer, but extend further into the flow. The ratio of the thicknesses of the streaming and Stokes layers is given by $\delta_s/\delta_1=\omega L/U_\infty$. We have assumed that the quantities $U_0(x)$ and $U_1(x)$ are of the same order and U_∞ is a typical representative value for both.

The relative thickness of the streaming layer then is:

$$\frac{\delta_s}{L}=R_s^{-1/2}=\left(\frac{\nu\omega}{U_\infty^2}\right)^{1/2}=\left(\frac{\omega L}{U_\infty}\cdot\frac{1}{R_0}\right)^{1/2} \quad (38)$$

For the types of flow considered here we were able to use uniform length and velocity scales throughout, that is, here $R_s=R_0$.

A final comment is appropriate here. The relative thicknesses of all three layers are independent of the amplitude parameter ϵ. The three sets of differential equations, therefore, can be solved consecutively in a system of coordinates that would appear most convenient for the problem.

V. Numerical Solution

The sets of differential equations of order ϵ^0, ϵ^1, and ϵ^2 are solved numerically in the two-dimensional space x-y. The method developed is not confined to any particular body configuration but the Howarth flow, that is, linear variation of the function $U_0(x)$ is chosen to facilitate comparison with earlier works. Such calculations were performed earlier for the equations of order ϵ and only for the velocity field by Ackerberg and Phillips.[9]

New dimensionless independent variables

$$\xi=x\omega/U_\infty,\quad \eta=y/2(U_\infty/\nu x)^{1/2},\quad \tau=t\omega \quad (39)$$

and new dimensionless dependent variables u^*, v^*, T^* are defined

$$u^*=\frac{u}{U_\infty},\quad v^*=\frac{v}{U_\infty}\left(\frac{U_\infty x}{\nu}\right)^{1/2},\quad T^*=\frac{T-T_\infty}{T_w-T_\infty} \quad (40)$$

An explicit marching technique is employed for numerical solution of the three sets of parabolic equations. Derivatives are expressed in terms of finite differences, first-order accurate in the ξ direction and second-order accurate in the η direction. A uniformly spaced mesh configuration is used in both the ξ and η directions. Nonetheless, the numerical results compare favorably with more sophisticated methods,[9,12] as described in Sec. VI.

The equations of mass and momentum are solved simultaneously. An iterative scheme is used to generate an initial profile. The same scheme is employed in order to proceed in the direction of increasing ξ. The temperature equation is linear and can be solved in a straightforward manner. The same method is used to solve the equations of order ϵ and ϵ^2.

VI. First-Order Approximation

Results of analytical or numerical calculations of this problem have appeared in numerous earlier publications.[4-6] We will confine ourselves to information that would require a different or novel interpretation, or to features of the flow that have passed unnoticed. Moreover, we will provide new results on the temperature field and the phenomenon of streaming. All the results pertain to a Howarth flow

$$U_0=1-b\xi$$

Different values of parameter b were used, covering the range from $b=-0.1$ to $b=0.1$.

The present numerical results were tested extensively against earlier analytical and experimental data. The agreement with the experimental data was found to be very good. An example of such a comparison is shown in Fig. 1. In this figure, we have collected the experimental and theoretical data of Hill and Stenning[19] and analytical results computed via the asymptotic method of Lighthill.[2] The present method seems to give the best agreement with the experimental data.

The wall value of the velocity phase angle is a characteristic feature that has been studied extensively. It represents the phase shift of the skin friction as compared to the outer flow fluctuations. Lighthill has indicated that this function grows almost linearly with ξ for small values and tends asymptotically to 45 deg for large values of ξ. We had earlier[13] calculated numerically the flowfields that correspond to all the intermediate values of ξ. In these earlier calculations, a coarse mesh configuration almost eliminated a peculiar feature of this property—the appearance of two points of inflection in the neighborhood of $\xi=1$. The results of our present calculations, depicted in Fig. 2, clearly exhibit this behavior in complete agreement with the earlier calculations of Ackerberg and Phillips.[9] Most recently, Cebeci and his coworkers[20] have arrived at similar results, solving numerically the equations in a three-independent variables domain. In the same figure, the maximum of the velocity overshoot is plotted. It is interesting to note that regardless of the pressure gradient this function starts from the value of 1.1 and attains a maximum in the neighborhood of $\xi=1$; that is, in the region where the skin-friction phase displays the peculiar dip

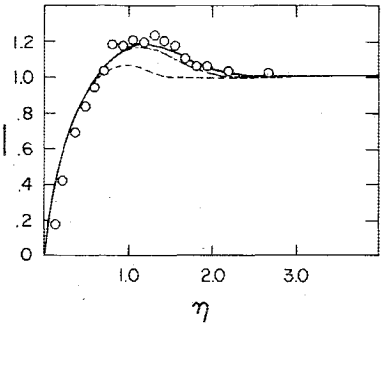

Fig. 1 Profiles of the amplitude of velocity oscillations at $\xi=2.844$ for $b\cong.035$.——, present method; o, —·—·—, experimental and numerical results of Hill and Stenning[19]; ---, calculated according to Ref. 2.

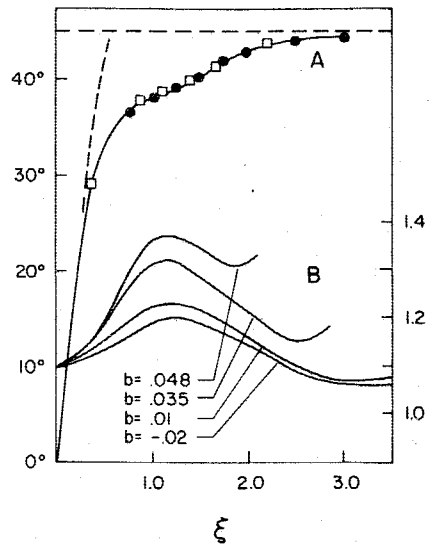

Fig. 2 The skin-friction phase shift, (curves A, scale on left); ---, Lighthill[2]; ◊, Ackerberg and Phillips[9]; ○, Cebeci[20]; ——, present method; and the maxima of the amplitude of velocity oscillations (curves B, scale on right).

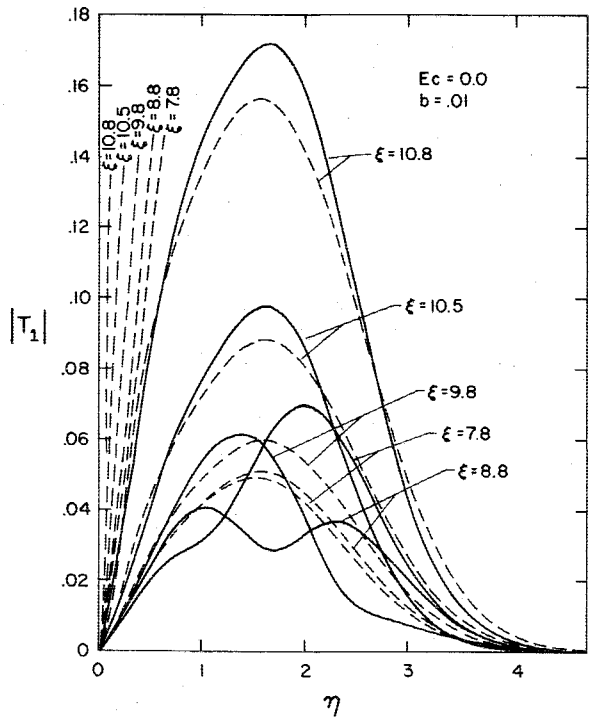

Fig. 3 Comparison of Lighthill's high-frequency approximation (— · — · —) with present numerical analysis (——).

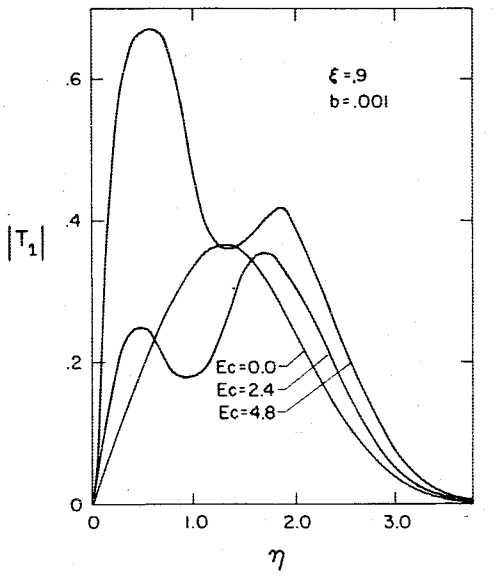

Fig. 4 Profiles of the amplitude of temperature oscillations for $T_I(\xi,0)=0$.

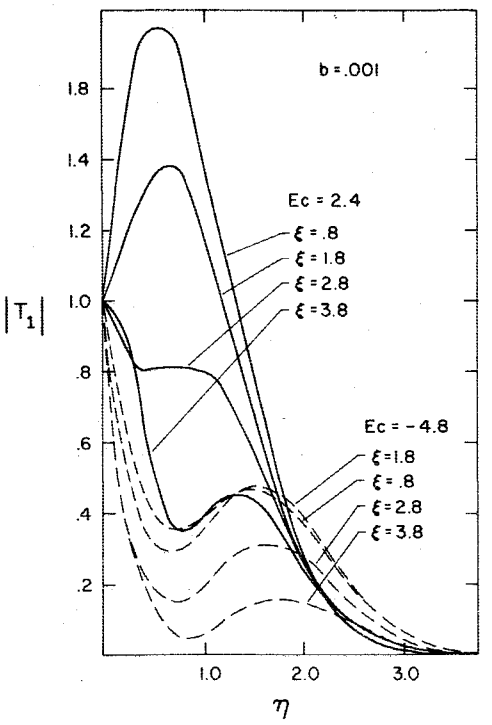

Fig. 5 Profiles of the amplitudes of temperature oscillations for $T_I(\xi,0)=1$.

described before. For larger pressure gradients, curves B in the figure appear to suddenly turn upward due to the fact that the separation singularity is approached.

Turning to the temperature field, our results are in excellent agreement with the asymptotic solution of Lighthill[2] for low frequencies. A figure giving this comparison may be found in Ref. 21, but is omitted here due to lack of space. For intermediate frequencies, no comparison is possible, since Lighthill's approximations hold for large or small frequencies only. For moderately large frequencies, the convergence of the asymptotic solution is rather slow and, in fact, it oscillates around the numerical solution as the parameter ξ grows. Such fluctuations are reminiscent of numerical instabilities but, in this case, are a feature of the solution. Similar undulations have indeed been observed in the velocity profiles.[9,10] Phillips and Ackerberg[10] have also indicated that the asymptotic results oscillate around the numerical results, if plotted against the frequency parameter.

A comparison of temperature profiles generated via Lighthill's asymptotic method and our numerical solution for high frequencies is shown in Fig. 3. Notice that the asymptotic profiles of Lighthill are well-behaved and have only one point of inflection. The exact numerical profiles, however, are wiggly and may possess three points of inflection. This behavior and the disagreement between the exact numerical solution and the asymptotic theory has been observed before in the velocity profiles[9,13] (see Fig. 1) and the phase advance[2,9] (see Fig. 2). In fact, this behavior is probably being inherited from the velocity field through the coupling of the equations. A better agreement of the numerical solution with the high-frequency asymptotic approximation would ob-

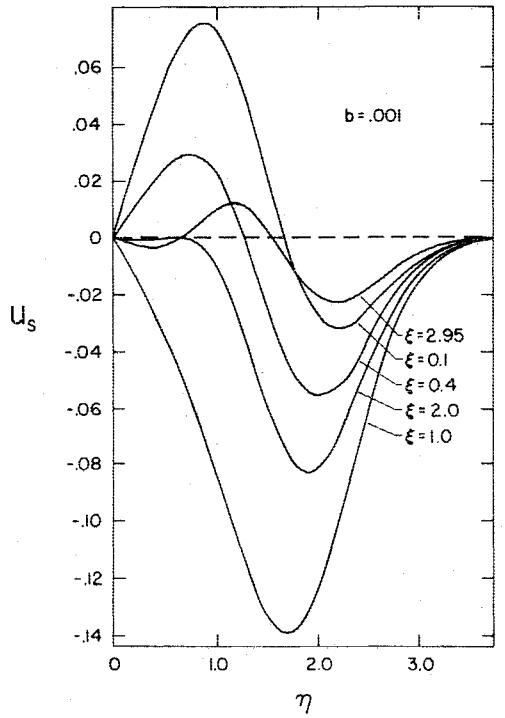

Fig. 6 Streaming velocity profiles.

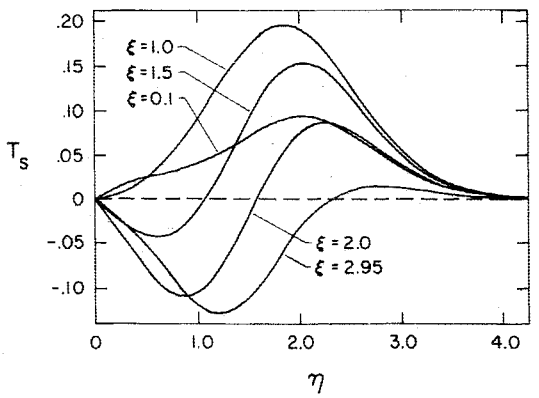

Fig. 7 Streaming temperature profiles for $Ec = 0.0$ (no dissipation).

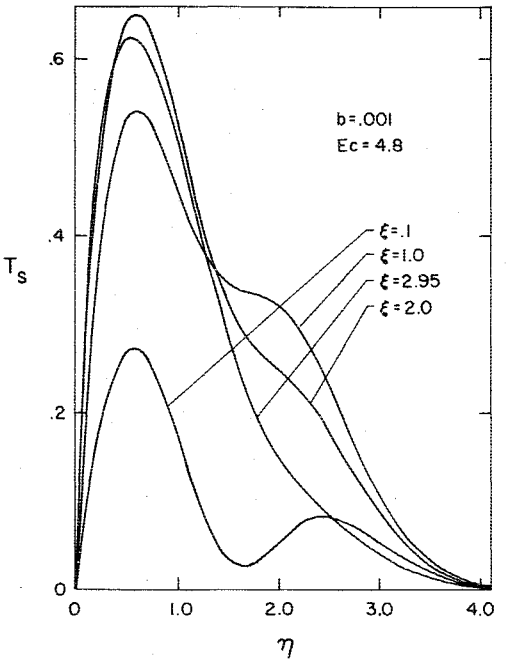

Fig. 8 Streaming temperature profiles for $Ec = 4.8$.

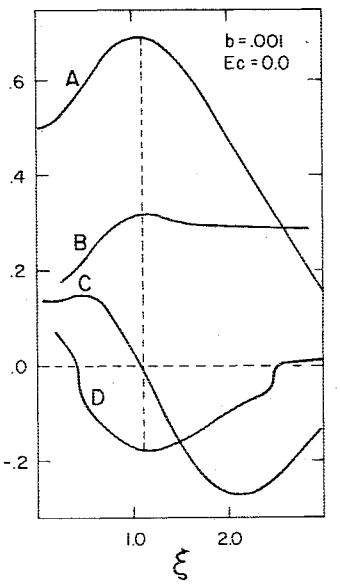

Fig. 9 The ratio $(\partial T_1/\partial\eta)/(\partial T_0/\partial\eta)$ at $\eta = 0$ (curve A); the maxima of temperature streaming $(T_s)_{max}$, (curve B); the ratio $(\partial T_s/\eta)/(\partial T_0/\partial\eta)$ at $\eta = 0$, (curve C); and the extrema of the velocity streaming, $(u_s)_{max}$ or $(u_s)_{min}$, (curve D).

viously be expected for larger ξ. However, for frequency parameters larger than 10, separation is approached for the mild adverse pressure gradients considered, and the disagreement is again bound to grow. For larger adverse pressure gradients, separation occurs for even smaller ξ's before the high-frequency region is reached. Finally, a physical interpretation is appropriate here. The sign of the fluctuating temperature gradient may change a few times across the boundary layer (Fig. 4). In fact these changes occur at distances from the wall, almost independent of the frequency or the Eckert number (Fig. 5). This implies that a certain amount of heat is shifted back and forth between the approximate locations $\eta = 1$ and $\eta = 2$, with the frequency of the externally imposed oscillations. It is interesting to note that the thickness of the zone in which heat transfer fluctuates in direction is not affected by the frequency parameter and the Eckert number.

VII. Second-Order Approximations

The streaming contribution to the velocity field is shown in Fig. 6, where the u_s profile is plotted for different values of the frequency parameter ξ. Positive and negative values of a profile indicate that the secondary streaming flow follows some kind of a recirculating pattern, similar to the ones observed by Schneck and Walburn[22] and Telionis and Romaniuk.[13] The magnitude of u_s at a given distance from the wall strongly depends on the value of ξ, and for $\xi \approx 1.10$, u_s reaches its largest value within the boundary layer. This phenomenon will be discussed later, together with the streaming effects on temperature.

Profiles of streaming for the temperature field, for the case of no dissipation, are shown in Fig. 7. It should be emphasized here that this represents a time-independent correction to the mean profile and the corresponding heat transfer represents a net gain or loss of heat. Depending on the value of the frequency parameter, the correction to the temperature field at a fixed distance from the wall may vary significantly and even change sign. For the case of no dissipation, the effect of "temperature streaming" on the wall heat transfer is very small, but it becomes quite significant for larger Eckert numbers. Figure 8 shows the streaming temperature profiles for $Ec = 4.8$. The effect of dissipation shifts the streaming temperature to larger and always positive values. The slopes at the wall also appear increased dramatically.

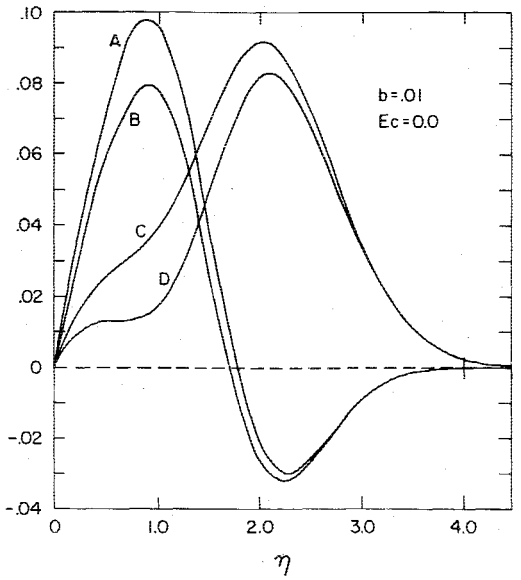

Fig. 10 The u_s and T_s profiles, (curves A and C, respectively); the u_s and T_s profiles corrected to $0(1/\epsilon^2 R_0)$, (curves B and D).

The relative effect of fluctuations on heat transfer is more clearly shown in Fig. 9, where the ratio of fluctuating and streaming components to the steady part of the heat transfer at the wall are plotted as functions of the frequency parameter ξ for the case of no dissipation. Extreme values of these parameters occur in the frequency region that was critical for velocity fluctuations, i.e., at about $\xi = 1.0$–1.2. While the fluctuating component of the wall heat transfer reaches a maximum there, the streaming part changes sign.

When the effect of dissipation is included, the values of heat transfer for both the fluctuating and steady streaming parts increase significantly, to reach values at least an order of magnitude larger than the values for $Ec = 0.0$. In Fig. 9, we also plot the extrema of streaming velocity and temperature profiles, defined simply as the largest positive or negative deviations from zero for fixed ξ. These quantities reach their own extrema again in the neighborhood of $\xi = 1.0$. This means that the "strongest" velocity and temperature streaming takes place for the intermediate value of the frequency parameter, at about $\xi = 1.1$. The T_s extrema decrease slightly to remain almost constant, i.e., independent of frequency for $\xi > 1.5$, as long as ξ is not close to its separation value.

From the u_s profile (Fig. 6) and the overall information given by Fig. 9, we can conclude that the steady streaming may either act so as to increase the mean flow rate through the boundary layer for very low and very high ξ, or to decrease it in the intermediate frequency range. Therefore, there would exist two transition regions, i.e., certain values of the frequency parameter for which the streaming flux will vanish altogether.

As mentioned before, the terms of order $1/R_0$ neglected in the $0(\epsilon^0)$ equations may become important in comparison with quantities $0(\epsilon^2)$, depending on the value of the parameter $k = 1/\epsilon^2 R_0$. Numerical results indicate that for $k = 10^{-5}$ the eventual correction is of the order of the truncation error and for $k = 10^{-4}$ it becomes quite significant. Figure 10 gives the comparison of the profiles of velocity and temperature streaming with and without the correction for this particular k at fixed ξ. In the region far from the wall, the influence of the correction is negligible, but quite large for intermediate and small values of η. The correction would become larger for larger k to eventually overpower the "pure streaming" itself.

It should be emphasized here that the streaming results reported were calculated for a very small pressure gradient, $b = 0.001$. They are driven by the terms resulting from the nonlinearity of the original equations and depend on u_1, v_1, and T_1. A well-known mechanism for driving streaming flows, as reported by Stuart,[4] is the pressure gradient terms, and this effect was practically eliminated here in order to isolate the influence of the nonlinearity. However, our calculations indicate that the magnitude of streaming terms, calculated with a reasonable pressure gradient ($b \approx 0.8$), is an order of magnitude bigger than the presented value.

Conclusions and Recommendations

A straightforward combination of a perturbation scheme and numerical analysis was proved to be an effective and accurate method for solving problems of oscillating boundary layers. Unlike earlier asymptotic techniques, the present method can handle arbitrary body configurations. Moreover, within the small amplitude approximation, it is far superior to the direct numerical solutions, because it requires integration in a two instead of a three coordinate space. The accuracy of the predictions was tested by extensive comparisons with earlier experimental and analytical data.

The effect of dissipation on fluctuations of the temperature field was investigated and it was found that it may generate temperature values and wall heat transfer rates twice as large as compared to the no dissipation values.

The nonlinear effects were examined for the first time for the velocity and the temperature fields. For very small pressure gradients, the order of magnitude of the streaming terms is rather small. It was shown that around the value 1.1 of the parameter $\omega x/U_0$, the streaming effects show the most characteristic changes. In fact, at $\xi \cong 1.1$ and for $Ec = 0$, the nonlinear steady contribution to the wall heat transfer vanishes and changes sign, but the fluctuating component of the same quantity attains its maximum. The streaming component of the velocity attains a minimum, which represents a steady flux in the opposite direction of the mean flow. Nonlinear effects, therefore, could be quite significant for intermediate values of the frequency parameter and for moderate or large values of the fluctuating part of the pressure gradient.

Acknowledgment

Research was sponsored by the Air Force Office of Scientific Research, Air Force Systems Command, USAF, under Grant No. AFOSR-74-2651D. The U.S. Government is authorized to reproduce and distribute reprints for Governmental purposes notwithstanding any copyright notation hereon.

References

[1] Moore, F. K., "Unsteady Laminar Boundary Layer Flow," NACA TN 2471, 1951.

[2] Lighthill, M. J., "The Response of Laminar Skin Friction and Heat Transfer to Fluctuations in the Stream Velocity," *Proceedings of the Royal Society*, Vol. 224A, 1954, pp. 1-23.

[3] Lin, C. C., "Motion in the Boundary Layer with a Rapidly Oscillating External Flow," *Proceedings of the 9th International Congress of Applied Mechanics*, Brussels, Vol. 4, 1956, pp. 155-169.

[4] Stuart, J. T., "Unsteady Boundary Layers," in *Recent Research of Unsteady Boundary Layers*, E. A. Eichelbrenner, ed., Vol. 1, 1971, pp. 1-46.

[5] Riley, N., "Unsteady Laminar Boundary Layers," *SIAM Review*, Vol. 17, Part 2, 1975, pp. 274-297.

[6] Telionis, D. P., "Calculations of Time Dependent Boundary Layers," in *Unsteady Aerodynamics*, R. B. Kinney, ed., Vol. 1, 1975, pp. 155-190.

[7] Rott, N. and Rosenweig, M. L., "On the Response of the Laminar Boundary Layer to Small Fluctuations of the Face-Stream Velocity," *Journal of Aeronautical Sciences*, Vol. 27, 1960, pp. 741-797.

[8] Illingworth, C. R., "The Effects of a Sound Wave on the Compressible Boundary Layer on a Flat Plate," *Journal of Fluid Mechanics*, Vol. 3, 1958, pp. 471-493.

[9] Ackerberg, R. C. and Phillips, J. H., "The Unsteady Laminar Boundary Layer on a Semi-Infinite Plate Due to Small Fluctuations in the Magnitude of the Free-Stream Velocity," *Journal of Fluid Mechanics*, Vol. 51, 1972, pp. 137-157.

[10] Phillips, J. H. and Ackerberg, R. C., "A Numerical Method for Integrating the Unsteady Boundary-Layer Equations when there are Regions of Backflow," *Journal of Fluid Mechanics*, Vol. 58, Pt. 3, 1973, pp. 561-579.

[11] Farn, C. L. S. and Arpaci, V. S., "On the Numerical Solution of Unsteady Laminar Boundary Layers," *AIAA Journal*, Vol. 4, April 1966, pp. 730-732.

[12] Tsahalis, D. Th. and Telionis, D. P., "Oscillating Laminar Boundary Layer and Unsteady Separation," *AIAA Journal*, Vol. 12, Nov. 1974, pp. 1469-1476.

[13] Telionis, D. P. and Romaniuk, M. S., "Nonlinear Streaming in Boundary Layer Flow," *Proceedings of 12th Annual Meeting of the Society of Engineering Science*, 1975, pp. 1169-1180.

[14] Moore, F. K. and Ostrach, S., "Displacement Thickness of the Unsteady Boundary Layer," *Journal of the Aeronautical Sciences*, Vol. 124, 1957, pp. 77-85.

[15] Ostrach, S., "Compressible Laminar Boundary Layer and Heat Transfer for Unsteady Motions of a Flat Plate," NACA TN 3569, 1955.

[16] Sparrow, E. M. and Gregg, J. L., "Nonsteady Surface Temperature Effects on Forced Convection Heat Transfer," *Journal of the Aeronautical Sciences*, Vol. 24, 1957, pp. 776-777.

[17] King, W. S., "Low Frequency, Large Amplitude Fluctuations of the Laminar Boundary Layer," *AIAA Journal*, Vol. 4, June 1966, pp. 994-1001.

[18] Telionis, D. P. and Gupta, T. R., "Compressible Oscillating Boundary Layers," *AIAA Journal*, Vol. 15, No. 7, July 1977, pp. 974-983.

[19] Hill, P. E. and Stenning, A. H., "Laminar Boundary Layers in Oscillatory Flow," *Journal of Basic Engineering*, Vol. 82, 1960, pp. 593-608.

[20] Cebeci, T., "Calculation of Unsteady Two-Dimensional Laminar and Turbulent Boundary Layers with Fluctuations in External Velocity," to appear in the *Proceedings of the Royal Society*, London.

[21] Telionis, D. P. and Romaniuk, M. S., "On the Response of Skin Friction and Heat Transfer to Fluctuating Boundary Layers," AIAA Paper 77-235, Jan. 1977.

[22] Schneck, D. J. and Walburn, F. J., "Pulsatile Blood Flow in a Channel of Small Exponential Divergence—II. Steady Streaming Due to the Interaction of Viscous Effects with Convected Inertia," *Journal of Fluids Engineering*, Vol. 98, 1976, pp. 707-714.